

<b>NIST Spectroscopy Beamline Suite: Hard X-ray Absorption Spectroscopy and Diffraction (4.5 keV to 40 keV 3-Pole wiggler source) Three-Letter Acronym (BMM - Beamline for Materials Measurement)</b>	
<b>Proposal Principle Team:</b> Daniel A. Fischer ( <i>Project Director and NIST Group Leader, <a href="mailto:dfischer@nist.gov">dfischer@nist.gov</a></i> ), Joseph Woicik and Bruce Ravel. ( <i>NIST Synchrotron Methods Group located at NSLS 631-344-5177</i> )	
<b>Science and Technology Advisory Panel</b>	
Simon Bare, <i>Senior Principal Scientist, UOP LLC, a Honeywell Company</i>	Bruce Bunker, <i>Professor, University of Notre Dame</i>
Steve Heald, <i>Group Leader/Senior Physicist, Advanced Photon Source</i>	Jean Jordon-Sweet, <i>Research Staff Member IBM</i>
Chi-Chang Kao, <i>Founding Director Joint Photon Sciences Institute (JPSI)</i>	Igor Levin, <i>Materials Research Engineer Chemistry Division, NIST</i>
Pat Lysaght, <i>Senior Member Technical Staff SEMATECH</i>	Ruben Reininger, <i>President Scientific Answers and Solutions Inc.</i>
Ian Robinson, <i>Professor University College London</i>	Wen-Li Wu, <i>NIST Fellow Polymers Division, NIST</i>

### **NIST NSLS-II Spectroscopy Beamline Suite: Materials Measurement to Promote Innovation and Industrial Competiveness**

Executive Summary: The National Institute of Standards and Technology (NIST) and the Department of Energy (DOE) have a 30 year ongoing partnership at the National Synchrotron Light Source (building to NSLS-II) developing advanced synchrotron measurement methods and delivering excellence in material science impacting important societal challenges in energy, health, environment, and national security improving our quality of life. This partnership promotes innovation and enhances US industrial competitiveness for inorganic and organic semiconductors, photovoltaics, SAMs, biological and environmental materials, batteries, catalysts, fuel cells, polymers, superconductors, ferroelectrics, and ferromagnets. Located at the NSLS, the NIST Synchrotron Methods Group of nine operates a suite of three state-of-the-art spectroscopy beamlines (U7A, X24A, and X23A2) that span the entire absorption-edge energy range of the periodic table to establish structure function relationships in advanced materials. More than 200 industry and academic researchers each year use the NIST Beamline Suite to accelerate the development of new materials into devices and systems with advanced functionality for a broad spectrum of industries. Building upon this success, NIST proposes to establish an NSLS-II spectroscopy suite of three state-of-the-art high throughput beamlines (with X-ray Diffraction capability) described in two beamline development proposals; Soft and Tender X-ray Spectroscopy and Microscopy (100 eV to 7.5 keV canted sources) and Hard X-ray Absorption Spectroscopy and Diffraction (4.5 keV to 40 keV three-pole wiggler source). Taken together, the NIST NSLS-II Spectroscopy Beamline Suite will be capable of measuring the electronic, chemical, and structural properties of almost any material, often at the nanoscale. NIST is committed to fully funding the construction of its proposed Spectroscopy Beamline Suite and to continuous world leading improvements in synchrotron measurement science and technology. Furthermore, NIST will build upon its NSLS based Synchrotron Methods Group to fully staff its stakeholder relationship in NSLS-II.

## A. Science Case: Hard X-ray Absorption Spectroscopy and Diffraction (4.5 keV to 40 keV)

In this proposal, we outline NIST's plans to develop an X-ray absorption fine structure beamline at NSLS-II using a three-pole wiggler source. The beamline will take advantage of the superior beam characteristics of the NSLS-II source for high resolution X-ray absorption spectroscopy (XAS) measurements. The beamline will also add new X-ray diffraction (XRD) capabilities to complement NIST's existing and planned XAS program. X-ray optics will be designed to provide either focused or collimated X-rays at the sample, for both high resolution XAS and diffraction experiments. The X-ray diffraction end station will be equipped to take advantage of the scanning capabilities of the beamline, adding glancing incidence XAS and XAS at constant  $q$  (reflectivity XAS and diffraction anomalous fine structure (DAFS)) to NIST's many other spectroscopic tools for materials science study. Polarization dependent XAFS measurements will also benefit from the high-precision eight-circle goniometer and its ability to accurately and quickly position samples relative to the X-ray beam.

This beamline will provide high-quality, high-throughput XAS for advanced sample characterization. XAS users will also have access to XRD for sample characterization. XAS and XRD are complimentary materials science probes. XAS measures local (short range) atomic structure while diffraction is more sensitive to a sample's long range order. By offering these combined and complementary measurement capabilities along with a variety of *in situ* sample environments, NIST's beamline will serve a broad range of structural characterization problems in materials science, ranging from the study of bulk mixed phases to epitaxy and strain state of thin films.

The XAS and XRD capabilities of the BMM beamline coupled with NIST's continuous development of automated high-throughput spectroscopy methods and world class high efficiency detectors will combine to have a large scale impact on the materials science of important societal challenges in energy, health, environment, and national security. Some strategic science case examples follow. They illustrate how this beamline will establish structure function relationships in advanced materials often at the nanoscale to accelerate the development of new materials into devices and systems with advanced functionality for promoting innovation and enhancing US industrial competitiveness.

### Science cases:

1. Local Structure and Phase Transitions in Electronic Ceramics, *I. Levin (NIST)*
2. Local Structure Function Properties of Strain Engineered Electronic Thin Films, *J.C. Woicik (NIST)*
3. Understanding Radiation Damage in Nuclear Materials with GA-XAS, *N. Hyatt, D. Reid, M. Stennet (U. Sheffield), B. Ravel, J.C. Woicik (NIST)*
4. *In situ* Characterization of Commercial Catalysts: From Understanding to Development, *S.R. Bare (UOP)*

Additional science Case Examples appear in the appendix starting on page 13

5. Proximity and Dimensionality Effects in Ferroelectric Nanostructures Studied by Diffraction Anomalous Fine Structure (DAFS), *J.C. Woicik (NIST)*
6. Local Structure Function Relationships in Thin Dielectric Films for Advanced Microelectronics, *P. Lysaght (SEMATECH)*
7. EXAFS of Phase Change Materials: Characterizing the role of the Local Bonding Environment on the Crystallization Properties of Chalcogenide Materials for Phase Change Memory Applications, *E. Joseph and J. Jordon-Sweet (IBM)*
8. High throughput XAS and an example of its application to chemical science, *B. Ravel, J.C. Woicik, D. Fischer (NIST), S.R. Bare, S.D. Kelly (UOP)*

## A.1: Local Structure and Phase Transitions in Electronic Ceramics

### I. Levin (NIST)

Exploitable properties of advanced electronic ceramics are intimately connected to fine details of atomic arrangements. Practical device applications require simultaneous optimization of several functional characteristics of these materials which is addressed via modifications of their crystal structures using complex chemistry. As a result, local atomic arrangements frequently deviate from those described by the average crystal structure; in many cases, such local deviations control the functional properties. Therefore, establishing comprehensive structure-property relations requires accurate knowledge of local structure details and understanding of the interplay between the local and average atomic arrangements. XAFS and diffraction are the main measurement tools for addressing this problem.

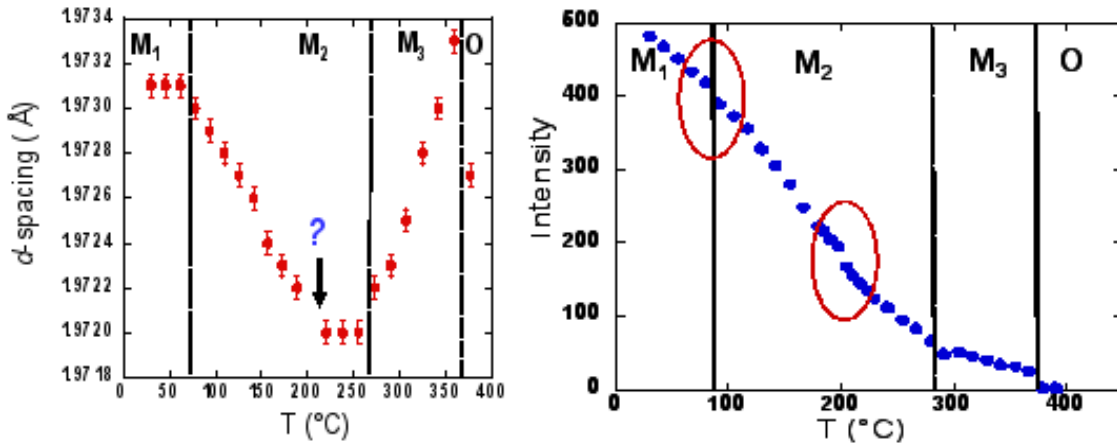


Figure 1: Temperature dependence of (left) 220  $d$ -spacing in  $\text{AgNbO}_3$  and (right) intensity of the superlattice reflection associated with ordering of Nb displacements. Phase transitions are indicated as well as some additional anomalies.

The NIST NSLS-II XAFS/Diffraction beamline will enable high-resolution X-ray diffraction combined with X-ray absorption spectroscopy in the *same* experiment. These measurements will permit simultaneous determination of the average structure and chemically-resolved local coordination using the same sample under identical environmental (temperature, atmosphere) conditions. Such combined measurements will greatly facilitate variable-temperature/controlled-atmosphere studies of structural changes by eliminating usual ambiguities associated with somewhat different sample environments in different experimental set-ups. Combining the two experiments will significantly decrease (by about a factor of two!) the overhead time associated with heating/cooling and equilibrating the sample at each temperature; this overhead becomes significant when a large number of temperatures is sampled. Additionally, the new beamline will drastically reduce both the time frame and the financial cost of these studies.

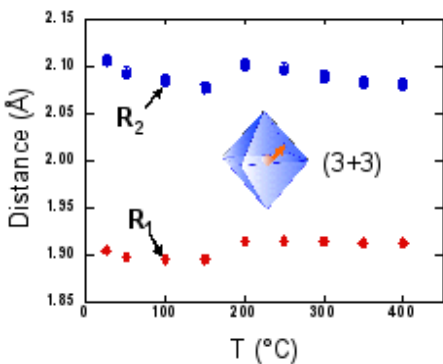


Figure 2: Temperature dependence of Nb-O distances extracted from Nb EXAFS. Local displacements of Nb are indicated. Note the anomaly around 200 °C which seemingly correlates with anomalies seen in diffraction (Fig. 1). Accurate knowledge of absolute temperatures in both experiments is necessary to ascertain these correlations.

One typical example of work that illustrates the potential benefits of the new facility is our recent study of local displacive order and its effect on the diffuse phase transition in  $\text{Ag}(\text{Nb,Ta})\text{O}_3$  dielectrics<sup>1</sup>.  $\text{Ag}(\text{Nb,Ta})\text{O}_3$  is the only known system that exhibits large temperature stable dielectric constants combined with modest dielectric losses at microwave frequencies. These remarkable properties have been attributed to a high-

<sup>1</sup> I. Levin, et al, *Phys. Rev. B.*, **79**:10, 104113 (2009)

frequency dielectric relaxation which yields a broad peak in the temperature dependence of dielectric constant. The peak has been traced to one (out of a sequence) of displacive phase transitions that occur in the end-member compound  $\text{AgNbO}_3$ . This transition is manifested by an abrupt increase in the splitting of certain Bragg peaks with no detectable changes in the space group symmetry. Our studies using a combination of several diffraction and spectroscopic techniques concluded that this transition reflects long-range ordering of local Nb displacements into an anti-polar array within the symmetry defined by the tilted  $[\text{NbO}_6]$  octahedral framework. A combination of average anti-polar Nb displacements and residual displacive Nb disorder explains a broad peak of dielectric constant and the underlying dielectric relaxation. The conclusions of our work suggested ways of synthesizing other systems with similar properties.

In this study, variable-temperature EXAFS and X-ray powder measurements provided key information on the nature of local Nb displacements and their ordering, respectively. These measurements were accomplished using two separate beam-lines at the APS (33-BM) and NSLS (NIST X23A2) that introduced temperature uncertainties between the two datasets and, therefore, complicated comparison of the results; furthermore, the necessity to coordinate these experiments at different facilities significantly delayed the completion of this study while doubling the travel costs. All these problems would be avoided with the new NSLS-II XAFS/Diffraction beamline.

## A.2: Local Structure Function Properties of Strain Engineered Electronic Thin Films

J.C.Woicik (NIST)

Strain engineering via epitaxial thin-film growth is an effective method by which the electronic and mechanical properties of a material may be custom tailored. Industrial applications range from enhanced electron mobility devices<sup>2</sup> to the recently demonstrated realization of ferroelectric memory conjoined with silicon<sup>3,4</sup>. Strain also alters both the nature and temperature of ferromagnetic, ferroelectric, and superconducting phase transitions.<sup>5</sup>

With the NIST NSLS-II XAS and XRD beamline, users will have the ability to combine high-resolution, polarization-dependent, near and extended x-ray-absorption fine-structure (XAFS) measurements with x-ray diffraction to determine the strain and local structural distortions in strained, epitaxial thin films grown on

substrates with dissimilar lattice constants. These measurements will have the goal of improving both first principles and phenomenological theoretical modeling of the unique structures and rich phase diagrams that these materials reveal.

As an example of our previous work, Figure 4 shows the polarization-dependent near edge XAFS spectra from a thin, 5 monolayer (2 nm)  $\text{SrTiO}_3$  film grown coherently on  $\text{Si}(001)$  by Motorola<sup>4</sup>. The enhancement of the pre-edge peak is direct evidence for the presence of a room-temperature ferroelectric polarization in the film normal to the film/substrate interface, and it is reproduced by *ab initio* density functional theory calculations of both the atomic and

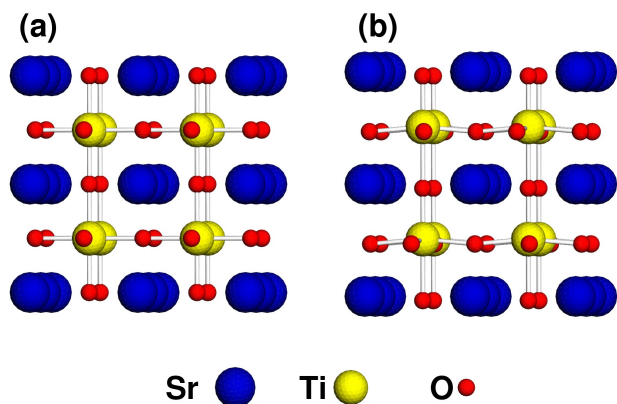


Figure 3: (a) Structure of cubic  $\text{SrTiO}_3$ . (b) Structure of strained  $\text{SrTiO}_3$  on  $\text{Si}(001)$  as calculated by DFT. The structure in (b) reveals both AFD and FE distortions.<sup>3</sup>

electronic structure of strained  $\text{SrTiO}_3$  (Figure 3). It should be noted that  $\text{SrTiO}_3$  is normally not ferroelectric at any temperature, so in essence the strain imposed on the film by the substrate has created a “new” and directly

2 M.L. Lee, et al., J. Appl. Phys. **97**, 011101 (2009).

3 J.C. Woicik, et al, Phys. Rev. B **75**, Rapid Communications, 140103 (2007).

4 M.P. Warusawithana, C. Cen, C.R. Sleasman, J.C. Woicik, Y. Li, L.F. Kourkoutis, J.A. Klug, H. Li, P. Ryan, L.-P. Wang, M. Bedzyk, D.A. Muller, L.-Q. Chen, J. Levy, and D.G. Schlom, Science **324**, 367 (2009).

5 D.G. Schlom, et al., Annu. Rev. Mater. Res. **37**, 589 (2007) and references therein.

observable phase of  $\text{SrTiO}_3$ . As a direct result of this research, Figure 5 demonstrates the first step towards the industrial “holy grail” of high-density, nano-sized, non-volatile ferroelectric memory; i.e., ferroelectric bits of memory written and read on a 2 nm  $\text{SrTiO}_3$  thin film on Si.

Note that the spectra shown in Figure 4 were collected at the NIST beamline X23A2 in a glancing-incidence, thin-film geometry to limit the X-ray penetration into the Si substrate. As X23A2 is not a focused beamline, each spectrum required 2 to 3 days (6 to 9 eight hour shifts) of beam time to obtain such high quality data. (EXAFS data to high  $k$  is a prerequisite for studying bond-length strain, and in fact it was not feasible to collect EXAFS from this thin film under current experimental conditions.) With the focused beam of the proposed NIST beamline and the higher flux of the NSLS-II three-pole wiggler, we anticipate an order of magnitude improvement in

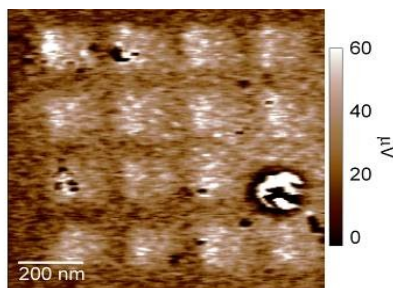


**Figure 5:** Ferroelectric bits of memory written and read by piezo-force microscopy at room temperature on a 2 nm  $\text{SrTiO}_3$  thin film grown coherently on Si.<sup>4</sup>

data collection time and hence throughput for such thin-film experiments. Additionally, we have recently demonstrated the superior performance of a new, state of the art Si drift detector commissioned at X23A2 that is capable of handling the increased count rates (to as high as 400,000 counts per second per detector element) expected at NSLS-II.<sup>6</sup> Thin-film research will therefore greatly benefit from the new NIST BMM.

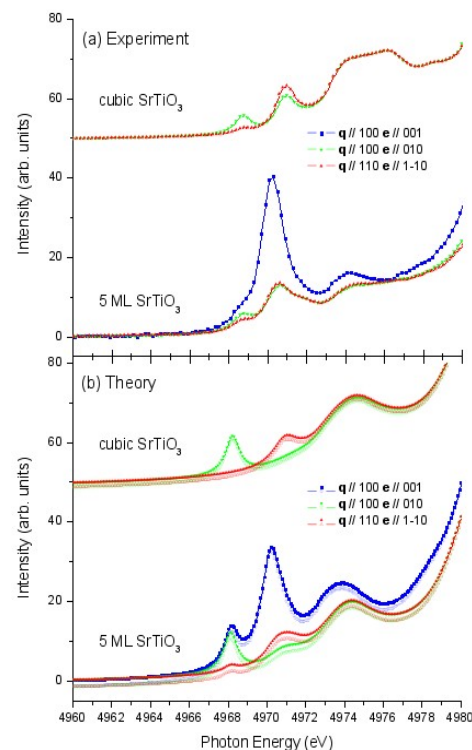


**Figure 4:** (a) Ti K near-edge spectra for cubic  $\text{SrTiO}_3$  and a 5 monolayer (2 nm)  $\text{SrTiO}_3$  thin film grown coherently on Si(001). (b) Theoretical spectra calculated<sup>3</sup> from the structures from Fig. 3.

### A.3: Understanding Radiation Damage in Nuclear Materials with GA-XAS

N. Hyatt, D. Reid, M. Stennett (U. Sheffield)  
B. Ravel, J.C. Woicik (NIST)

A legacy of the civil and military fuel cycles in the UK and elsewhere is a stockpile of separated plutonium which constitutes a considerable proliferation and security risk. Ultimately, a fraction of this stockpile will require immobilization in a durable and passively safe matrix, suitable for final disposal. A key element of the disposal system safety case is reliable prediction of the evolution of the immobilization matrix under the influence of radiation damage arising from actinide  $\alpha$ -decay which, eventually results in a crystalline to amorphous phase transition. Our study<sup>7</sup> using Grazing Angle XAS (GA-XAS) on beamline X23A2 at the NSLS is the first to quantify the effect of radiation damage on the co-ordination environment of key elements in model immobilization systems such as zirconolite –  $\text{CaZrTi}_2\text{O}_7$ .

**Method development at NSLS X23A2:** To simulate radiation damage caused by  $\alpha$ -recoil in model immobilization ceramics, we use 2 MeV  $\text{Kr}^+$  implantation which results in a fully amorphized surface layer about 1  $\mu\text{m}$  in thickness, Fig 6.

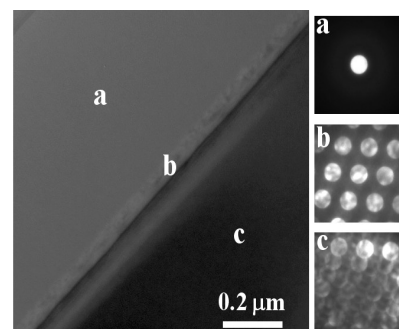


**Figure 6:** cross sectional TEM image and ED patterns of  $\text{Kr}^+$  implanted  $\text{CaZrTi}_2\text{O}_7$ , showing a) amorphized surface layer; b) partially damaged zone; and c) undamaged interior.

<sup>6</sup> J.C. Woicik, B. Ravel, D.A. Fischer, and W.J. Newburgh, *J. Synch. Rad.* **17**, 409 (2010), [doi:10.1107/S0909049510009064](https://doi.org/10.1107/S0909049510009064)

<sup>7</sup> D.P. Reid, et al, Nuclear Instruments and Methods in Physics Research, **B268** (2010) 1847, [doi:10.1016/j.nimb.2010.02.026](https://doi.org/10.1016/j.nimb.2010.02.026)



Consideration of X-ray penetration depth shows that even at the Ti K edge, XAS data acquired in conventional 45° fluorescence mode are dominated by sampling of the undamaged interior of the specimen. However, by careful selection of the incident grazing angle, XAS data are acquired only from the radiation-damaged surface layer. Ti K-edge XANES are especially sensitive to the local symmetry of Ti, Fig. 7.

Analysis of the height and position of this feature<sup>8</sup> confirms a transformation to ~100% 5-fold coordination in the damaged surface layer, compared to the crystalline pristine material which contains both 6- and 5-fold coordinate Ti in the ratio 2:1, Fig 8.

Quantitative analysis of EXAFS data<sup>9</sup> measured in this geometry confirmed the XANES analysis. Following sample irradiation, EXAFS data show a loss of fine structure consistent with the loss of long range periodicity, Fig. 9. The FT  $\chi(k)$  show a near complete suppression of signal beyond the first shell, consistent with the loss of long range periodicity. GA-XAS spectra acquired from 2 MeV Kr<sup>+</sup> irradiated zirconolite were found to be

indistinguishable from that acquired from a fully radiation amorphized (i.e. metamict) zirconolite mineral (dated to > 500 Ma).

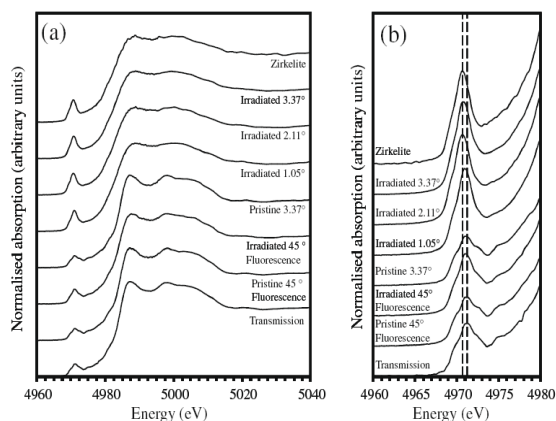


Figure 7: a) Ti K edge XANES spectra of zirconolite acquired in transmission and fluorescence mode (at varying angles of incidence); (b) detail of pre-edge XANES feature.

Crucially, this will enable the study of radiation damaged materials for which no natural mineral analogues exist.

**NSLS II XAFS Beamline:** Future development of this methodology will benefit significantly from the capabilities of the proposed NSLS II XAFS beamline:

**Improvement in flux by an order of magnitude** compared to NSLS X23A2 due to use of focusing optics, which will reduce data acquisition time from >6 h per EXAFS data set, to ~1 h using a state of the art Si drift detector. This development will assist our research in four ways:

- Higher sample throughput, enabling the structure of damaged materials to be determined e.g. as a function of dose, composition etc.
- Use of smaller specimens and consequent cost savings: presently each experiment uses an 18 mm ceramic disc, ion implanted at a cost of \$1000.
- Acquisition of data from dilute dopant absorbers which can have a strong effect on radiation damage tolerance.
- Potential for novel *in situ* measurement of recrystallization kinetics and speciation using a high temperature stage at grazing angle.

<sup>8</sup> F. Farges, R.C. Ewing and G.E. Brown Jr., Journal of Materials Research, **8** (1993) 1983.

<sup>9</sup> Ravel and M. Newville, Journal of Synchrotron Radiation 12 (2005) 537, [doi:10.1107/S0909049505012719](https://doi.org/10.1107/S0909049505012719)

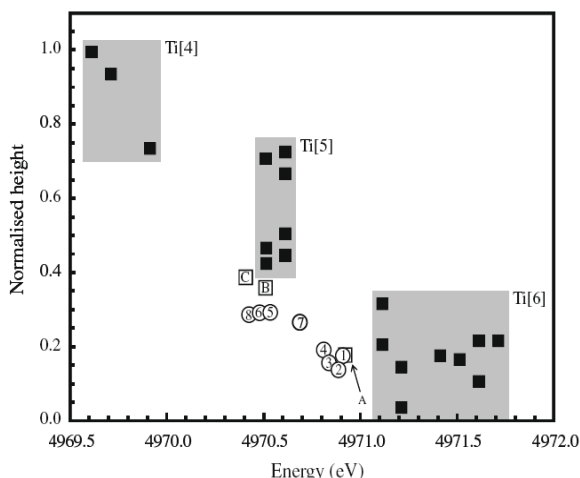


Figure 8: Correlation between Ti co-ordination environment and normalized height and energy position of pre-edge feature in Ti K edge XANES spectra. Solid squares are data from Ti bearing model compounds reported by Farges; open squares are data reported by Farges for re-crystallized metamict zirconolite (A), and metamict zirconolites (B and C).<sup>8</sup> Open circles show data from this study for: pristine zirconolite in transmission (1) and in fluorescence mode with  $\alpha = 45^\circ$  (2), and  $\alpha = 3.37^\circ$  (3); and irradiated zirconolite in fluorescence mode at  $\alpha = 45^\circ$  (4),  $\alpha = 3.37^\circ$  (7),  $\alpha = 2.10^\circ$  (6),  $\alpha = 1.10^\circ$  (5); also shown are data acquired in fluorescence mode for natural metamict zirconolite (zirkelite) (8).

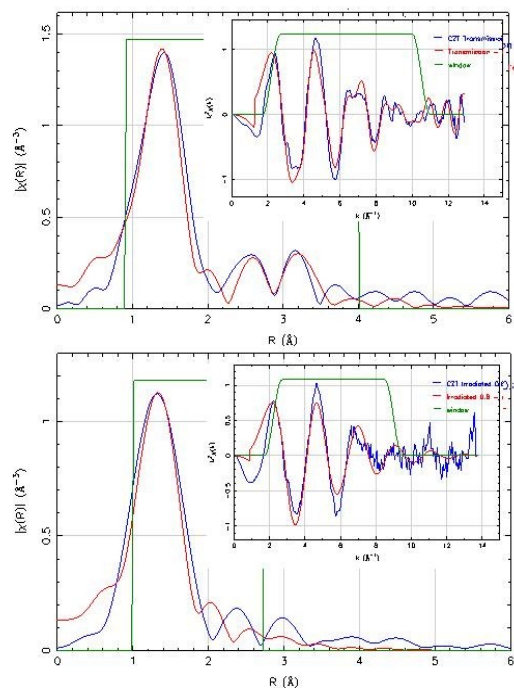


Figure 9: FT  $\chi(k)$  and  $k^2\chi(k)$  data (inset) for pristine (top) and 2 MeV Kr+ amorphized (bottom)  $\text{CaZrTi}_2\text{O}_7$ ; data in blue and fit in red; data collected in transmission and grazing angle mode, respectively.

Acquisition of good quality EXAFS data to high  $k$  is essential to determine accurate metal-oxygen contact distances and the potential presence of intermediate range order.

**High energy resolution** using a Si(311) monochromator is essential to resolve subtle changes in XANES features as seen in this study as a consequence of radiation damage (Fig 7).

**An eight circle goniometer** will enable improved reproducibility and accuracy in alignment of samples at grazing angle, enabling automation of sample measurements and application of this method by new and inexperienced users. A dedicated goniometer is also key to combining GA-XAS with *in situ* techniques.

#### A.4. In situ Characterization of Commercial Catalysts: From Understanding to Development

S.R. Bare (UOP LLC, a Honeywell Company)

UOP LLC, headquartered in Des Plaines, IL, USA, is a leading international supplier and licensor of process technology, catalysts, adsorbents, process plants, and consulting services to the petroleum refining, petrochemical, and gas processing industries. UOP is a wholly-owned subsidiary of Honeywell International, Inc. and is part of Honeywell's Specialty Materials strategic business group. UOP has been using synchrotron radiation primarily to probe the structure of its catalysts and adsorbents since the early 1980's and was a charter member of the original Matrix PRT at the NSLS in the mid-1980's. UOP is currently a member of MR-CAT at the APS and a member of the SCC at the NSLS and has collaborated with NIST at the NSLS for many years. ***This collaboration is essential; we anticipate full utilization of the world-class capabilities of BMM.***

***UOP fully supports the development and construction of the BMM beamline by NIST. The capabilities envisioned for this beamline are focused on both fundamental understanding and also materials***

**measurement. As such it will provide new insights into catalyst structure and function leading to development and implementation of new breakthrough catalyst systems.**

The successful commercialization of a catalyst involves many different steps from the initial discovery, to scale-up and manufacturing, and finally to commercial service. The use of X-ray absorption spectroscopy (XAS) to provide local chemical and structural information of a particular element in a catalyst is a technique of choice at UOP for all steps in this process. The well-known strengths of XAS are fully utilized, particularly the *in situ* methodology. The envisioned capabilities of BMM will fully meet the needs of such a catalyst development program and greatly expand on the current capabilities at, for example, the NIST beamline X23A2 at the NSLS.

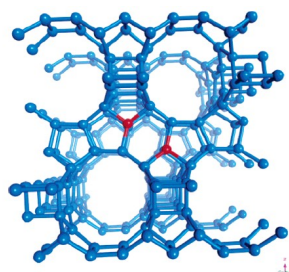


Figure 11: Representation of the Sn-beta zeolite structure as derived from the EXAFS data, viewed along the b-axis (for clarity the oxygen atoms are not shown). The only Sn distribution consistent with the EXAFS data is one where pairs of Sn atoms occupy opposite vertices of the six-member rings. A pair of T5 sites (red), with the required 5.1 Å separation is shown, representing one possible Sn-pair within the Beta-zeolite structure. This Sn pair distorts two of the 12-membered ring channels as viewed from the [100] direction and all four 12-membered ring channels as viewed from the [010] direction.

typically low concentration of heteroatom in such catalysts.

After a catalyst is developed and progresses from laboratory-scale (tens of grams of material) to scale-up where Kg quantities are produced to manufacturing where the unit is now tons - then the emphasis shifts from fundamental understanding to rapid commercialization, where throughput (productivity) and turnaround time (direct relevance) are key drivers. At this stage often subtle changes in formulation or preparation conditions results in a change of catalyst performance. The ability to detect any structural changes is critical to having an impact on a catalyst development program, where a correlation can be made to conversion and selectivity. The recent combined development between NIST, UOP, and BNL of a four-

One goal of catalysis science is to develop catalysts that are 100% selective to the desired product leading to an energy efficient process. The substitution of a heteroatom into a zeolite has been shown to provide new functionality of the material leading to new applications, often providing isolated active sites that are indeed 100% selective<sup>10</sup>. In such a catalyst there are several fundamental questions that need to be answered: (1) Does the heteroatom substitute into the framework? (2) Does it exist as an extra-framework species? (3) What is the crystallographic location of the atom in the unit cell? EXAFS is an ideal technique for resolving such questions. EXAFS was successfully used to show that the substitution of Sn into the  $\beta$ -zeolite structure leads to the formation of a unique paired Sn site (Fig. 11) that is believed to give rise to the unique 100% selectivity of this catalyst for many oxidation reactions<sup>11</sup>. By understanding the atomic-level details of such catalysts, insight is gained that can be applied to the development of other catalyst systems. We envision using *in situ* XAS to probe the structure of many similar heteroatom-substituted zeolites at BMM. Here, however, advantage will be made of using both the XRD and XAS - so both the local and long range structure will be elucidated. This is particularly important in zeolitic materials where it is known that the zeolitic structure can be damaged due to processing conditions such as steaming or high temperature operation. Moreover, the suite of advanced detectors will ensure that high quality XAS data can be collected from the

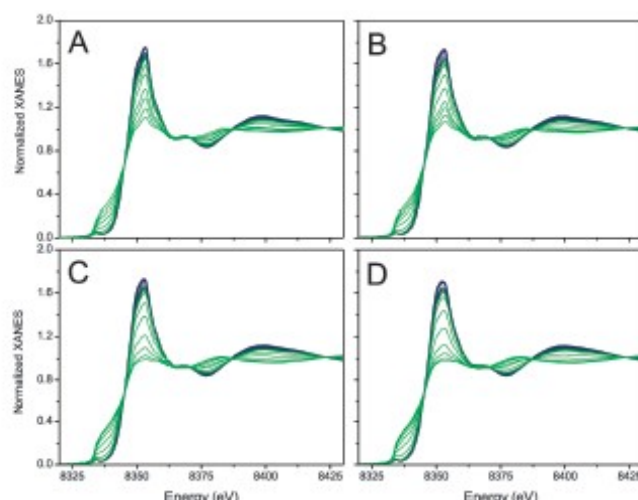


Figure 10: Simultaneous normalized Ni K-edge TPR-XANES data of Ni-containing catalysts. Prep1 (A); Prep2 (B); Scale up (C), and Lab Prep (D).

10 Corma, A.; Nemeth, L.T.; Renz, M.; Valencia, S. *Nature* **2001**, 412, 423-425.

11 S.R. Bare, S.D. Kelly, W. Sinkler, J.J. Low, F.S. Modica, S. Valencia, A. Corma, L.T. Nemeth, *J. Am. Chem. Soc.* **127** (2005) 12924-12932.



channel ionization chamber for XAS measurements, combined with the appropriate in situ reactor have revealed that such subtle structural changes can be measured in fully-formulated commercial catalysts<sup>12</sup>. Fig. 10 shows the Ni K-edge XANES spectra of four catalysts obtained simultaneously using this new instrumentation. The data reveal differences in the reducibility of the Ni which is thought to be a measure of the final catalyst activity. Such methodology will be utilized at BMM along with the increased flux, the advanced control and data management/processing, and the enhanced energy resolution of the Si(311) monochromator.

## B. Beamline Concept & Feasibility

The NIST Beamline for Materials Measurement (BMM) is a facility primarily for efficient, high-throughput X-ray Absorption Spectroscopy (XAS) with an additional mission to high-quality X-ray Diffraction (XRD) for materials measurement. The BMM is for an NSLS-II three-pole wiggler source and is designed to operate in the range from 4.5 keV to 40 keV. Initial optics designs were commissioned by NIST from IDT, Ltd. Design work will continue under a contract with Reuben Reininger (Scientific Answers & Solutions).

### B.1 Optical design

The first optical element will be a vertical *and* horizontal collimating (VHC) mirror with stripes of different optical coatings along its length. Use of two coatings allows for optimized performance throughout the entire energy range for XAS. The mirror will be mounted on a hexapod system that will perform the translations and roll required to position the chosen optical stripe on the beam. Note that NIST will be awarding a contract to build this mirror in FY11 and expects delivery by FY12. We will place this mirror inside the shield wall at 14 meters from the source to collect a larger swath of beam thereby maximizing flux at the sample.

The first optical enclosure (FOE) houses the following major optical elements:

1. A double crystal monochromator, shown in Fig. 12 with both parallel and perpendicular motion of the second crystal allowing for fixed exit operation. Both Si(311) and Si(111) crystals are available, although the crystal cage only seats one crystal set at a time. Normal operation will use the Si(311) crystals, as their superior energy resolution is a significant benefit for high resolution XAS studies. NIST procured this monochromator from FMB Oxford in early FY10 and is currently commissioning it at NSLS beamline X7A.
2. Two mirrors bendable along the meridional direction: a sagittal cylinder and a plane mirror. The sagittal cylinder will have the same optical coatings as the VHC first mirror and will be used to obtain either a beam focused both horizontally and vertically or only horizontally for use in XAS and XRD experiments, respectively. The flat will be used for asymmetric XRD experiments and when bent along the vertical direction for high throughput XAS. Procurement of these mirrors is expected in FY11 with delivery in FY12.
3. Other optical elements, including a photon shutter, white beam slits, various masks and monochromatic slits, and an extensive complement of diagnostic equipment.

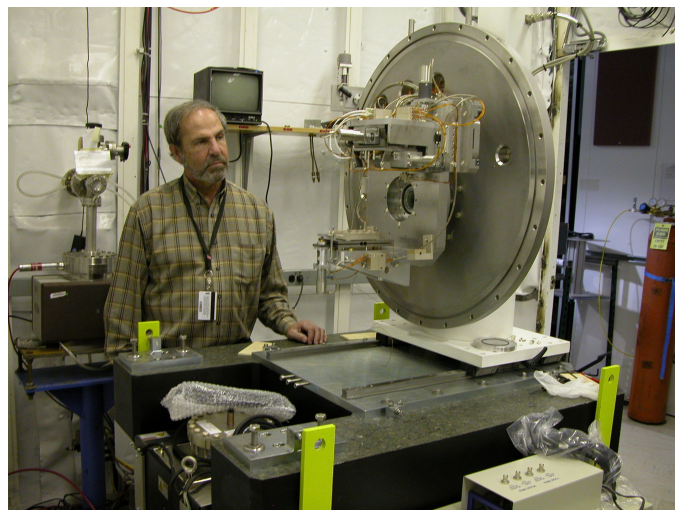


Figure 12: NIST DCM in the X7A hutch where it is currently being commissioned.

12 S.R. Bare, S.D. Kelly, B. Ravel, N. Greenlay, L. King, G. Mickelson, *Physical Chemistry Chemical Physics*, 2010, DOI: 10.1039/b926621f.

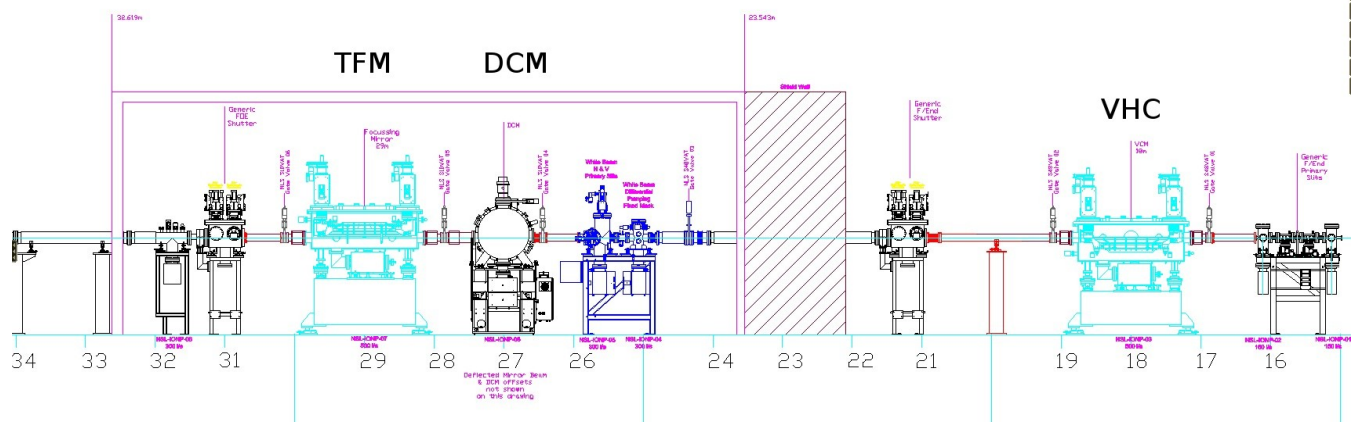


Figure 13: Schematic layout of the BMM optics. Note that the VHC is placed inside the shield wall to maximize both vertical and horizontal aperture that can be collected. The DCM, TFM, and other components are in the FOE.

## B.2 End-station design

The end station consists of a single hutch with an optical table housing an additional harmonic rejection mirror, a conventional XAS setup, and an eight circle goniometer. The XAS station includes ionization chambers, energy discriminating fluorescence detector, and sample stage along with adequate room for additional user instrumentation. The goniometer is used for high resolution XRD measurements as well as XAS experiments in glancing angle, total reflection, and polarization-dependent XAS geometries, in addition to diffraction anomalous fine structure (DAFS). Services (power, signaling, water, gas handling, and so on) are tightly integrated into the experimental station in service of efficient, high-throughput XAS and XRD.

Much instrumentation for the XAS station – including silicon drift detectors, ionization chambers, sample stages, a cryostat, a VME-based control system, computing and communication hardware, and so on – is available for transfer from NIST's current XAS beamline, X23A2. Most of this hutch equipment is new, some items (cryostat, VME system) were obtained in FY10.

## C. Required Technical Advances (if any)

- Clear description of properties of the three-pole wiggler and the layout of the front-end so that optics can be properly designed.
- Multi-element Ge drift detector for higher energy XAFS (current R&D effort in collaboration with BNL Instrumentation).

## D. User Community and Demands

BMM replaces and expands upon the user program already in place at NIST's beamline X23A2. For the current cycle (May-August 2010), 24 general user requests competed for only 8 slots under our PRT contribution to the GU program. For this upcoming time period (September-December 2010), there are 21 requests. In Table 2 on page 22, we summarize our user program from recent years; i.e., all general users and PRT users (including NIST scientists not stationed at NSLS) other than local staff. Between current demand, the consolidation of the NSLS XAS program into a smaller number of beamlines at NSLS-II and NIST's new capability for XRD measurements this beamline will quickly become fully subscribed. 38% of visits to X23A2 (see Table 2) are by industrial users, consistent with NIST's mission of service to U.S. industrial competitiveness. Note also the large number of repeat visitors, indicating the level of service and performance our users enjoy.

Statistics from the NSLS User Administration office show that X23A2 is oversubscribed in the General User program by almost a factor 2 (based on days requested compared to days available). The XAS General User program in aggregate at NSLS is similarly oversubscribed. Given the certain reduction in number of conventional XAS beamlines at NSLS-II relative to the size of the program at NSLS, NIST BMM will be required to accommodate a considerably larger user base, even when compared to the larger fraction of General

User time under the new access policy. Furthermore, current NIST users and local NIST PRT staff will apply for beamtime through the GU program, further increasing GU demand.

Brookhaven National Laboratory hosts the Joint Photon Science Institute (JPSI), which brings together Industry, National Laboratories, and Universities to catalyze innovation using synchrotron radiation at NSLS-II. NIST is a founding member of JPSI and Dr. Chi-Chang Kao is the Director (and a member of this proposal's Science and Technology Advisory Panel). Over the past year, JPSI has held NSLS/NSLS-II New Opportunity Workshops in Microelectronics, Batteries, and Photovoltaics. Each of these workshops has brought together technology and academic leaders (total of 150) who see NIST's proposed NSLS-II spectroscopy beamlines as an important key to solving some of the Nation's most challenging problems (see attached JPSI letter of endorsement from Dr. Chi-Chang Kao in the appendix, page 23).

## E. Proposal Team Expertise and Experience

The Proposal Principal Team Daniel Fischer (project director), Joseph Woicik, and Bruce Ravel are members of NIST's Synchrotron Methods Group of 9 staff (all located at the NSLS full time, Fischer is the group leader) that currently run 3 NIST PRT Spectroscopy Beamlines (U7A, X24A, X23A2) and 2 NIST Measurement and Instrument Development Team (MIDT) Beamlines for each of the NIST' NSLS-II microscope development projects. These NIST staff members represent a permanent and growing investment by NIST in developing and operating beamlines at NSLS-II (Type-II beamline development). Fischer, Woicik, and Ravel are senior members of the technical staff and are all highly regarded scientists within the NIST institution. The Proposal Principal Team has significant and highly successful direct beamline experience building, developing, maintaining, and managing spectroscopy user facilities, continuously improving measurement capabilities, and producing excellent science spanning nearly three decades. They are all highly respected members of the synchrotron community and are valued NIST ambassadors to the DOE at the NSLS (and NSLS-II). The team often represents the user community on the NSLS User Executive Committee and numerous NSLS and DOE advisory teams and review panels. A one page brief bio of each Principal Proposal Team member appears in the appendix (see page 24).

## F. Suggestions for BAT Membership

See the Science and Technical Advisory Panel list on page 1 of this proposal.

## G. Funding and Management

<b>NIST NSLS-II Hard XAS and Diffraction Total Capital Investment to Date</b>	<b>\$872K</b>
Existing FMB Oxford Water Cooled Double Crystal Monochromator	\$500 K
Existing X23A2 4-Element Si Drift Detector	\$130 K
Existing Low Vibration 4 °K High Temperature He Cryostat	\$70 K
Existing X23A2 Pulse Counting Electronics	\$50 K
Existing X23A2 Sample Stage	\$30 K
Existing X23A2 Harmonic Rejection Mirror	\$22 K
Existing X23A2 Glancing Incidence Stages	\$20 K
Existing X23A2 Single Element Si Drift Detector	\$20 K
Existing X23A2 Ion Chambers	\$15 K
Existing X23A2 EXAFS Table	\$10 K
Existing X23A2 Heald/Stern/Lytle Detector	\$5 K

**NIST NSLS and NSLS-II Funding and Staffing Overview:** NIST is committed to fully funding the construction of its proposed NSLS-II Spectroscopy Beamline Suite and to continuous improvements in synchrotron measurement science and technology to keep them world-leading. NIST will build upon its NSLS based Synchrotron Methods Group to fully staff our stakeholder relationship in NSLS-II to develop the proposed NSLS-II Spectroscopy Beamline Suite.

**NIST NSLS-II Beamline Development Approach Overview:** (1) Finish optical design and specification of all mirrors. (2) Develop a detailed beamline conceptual design including cost and schedule. (3) Develop a beamline organizational and management system. (4) Develop a full Beamline Project Execution Plan in coordination with NSLS-II management and staff.

**NIST Transition Plan to NSLS-II Overview:** (1) Maintain NIST's leading role in synchrotron materials measurement science together with our partners as fully committed long time stakeholders at the NSLS moving to an operational NSLS-II. (2) As soon as possible, begin assembling and commissioning on the floor of NSLS-II a new NIST spectroscopy beamline suite teaming with expert contractors to leverage our NIST group at NSLS. (3) Strategically move NIST's NSLS state-of-the-art endstations to their new NIST NSLS-II beamlines, thereby minimizing down time.



## Appendix A: Additional science cases

### A.1. Proximity and Dimensionality Effects in Ferroelectric Nanostructures Studied by Diffraction Anomalous Fine Structure (DAFS)

J.C. Woicik (NIST)

The great sensitivity of ferroelectrics to chemistry, defects, electrical boundary conditions, and pressure arises from the delicate balance between the long-range Coulomb forces that favor the ferroelectric state and the short-range repulsive forces that favor the non-polar cubic structure.<sup>13</sup> It is therefore not surprising that the magnitude and direction of a ferroelectric polarization as well as its critical temperature depend strongly on the size and shape of the crystal.<sup>14</sup> Recently, it has been demonstrated that, in analogy to a superconductor placed in contact with a normal metal, ferroelectrics also exhibit “proximity” effects; i.e., a paraelectric can become a ferroelectric when sandwiched in a superlattice with a true ferroelectrics, and this phenomenon also couples with coherency strain.<sup>15</sup>

In order for nano-ferroelectrics to realize their full potential in the micro-electronics industry, phenomenon intrinsic to ferroelectricity must be explored and understood on the nano-scale. However, it is nearly impossible to isolate the electrical response of a ferroelectric nano-structure in close proximity to either another nano-structure or a substrate. This is because electrical measurements must be made on a sandwich structure consisting of two electrodes around a dielectric,<sup>16</sup> and the electrical measurement, if possible, would measure the polarization of the entire sample. As examples, “self assembled” ferroelectric quantum dots are fabricated either by Stransky-Krastonov growth leaving several wetting layers, or are crystallized from melts leaving contact with their host matrix. Additionally, superlattice structures often contain layers with the same element, and the use of ion beams or atomic-force microscopy to cut nano-ferroelectrics leaves remnant, non-nano-patterned material.

X-ray absorption fine structure (XAFS) is ideally suited to study the class of ferroelectrics known as perovskites because the x-ray absorption near-edge structure of the transition metal has a signature unique to the ferroelectric polarization that determines both its magnitude *and* direction, and hence phase.<sup>17</sup> However, due to the “common-element” problem; i.e., the non-selective XAFS averaging of all absorbing atoms in the probing volume, it is impossible for XAFS itself to isolate this signature from many of the typically fabricated nano-structures.

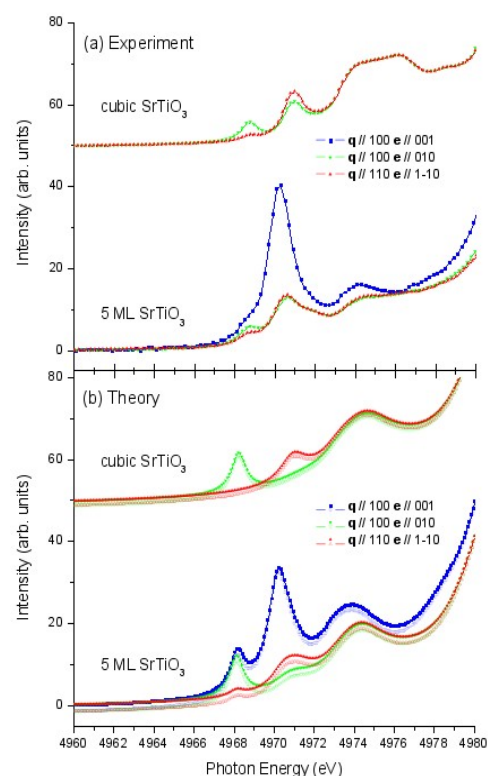


**Figure 14:** Ti K x-ray absorption fine structure spectra from cubic SrTiO<sub>3</sub> and from a thin (~ 2 nm) SrTiO<sub>3</sub> film grown coherently on Si(001). The spectroscopic ferroelectric signature of the film; i.e., dipole allowed Ti 1s to Ti 4p transitions (blue curve), occurs at 4970 eV. Note that its polarization dependence of the feature w/r to the incident photon beam indicates that the direction of the spontaneous polarization in the film is along the surface normal (top experiment; bottom theory)<sup>18</sup>

<sup>13</sup> R.E. Cohen, *Nature* **358**, 136 (1992).

<sup>14</sup> *Introduction to solid state physics*, C. Kittel, 5<sup>th</sup> edition, John Wiley and Sons, New York (1976).

<sup>15</sup> D.G. Schlom, L.-Q. Chen, C.-B. Eom, K.M. Rabe, S.K. Streiffer, and J.-M. Triscone, *Annu. Rev. Mater. Res.* **37**, 589 (2007), and references therein.

<sup>16</sup> J.F. Scott, *Science* **315**, 954 (2007).

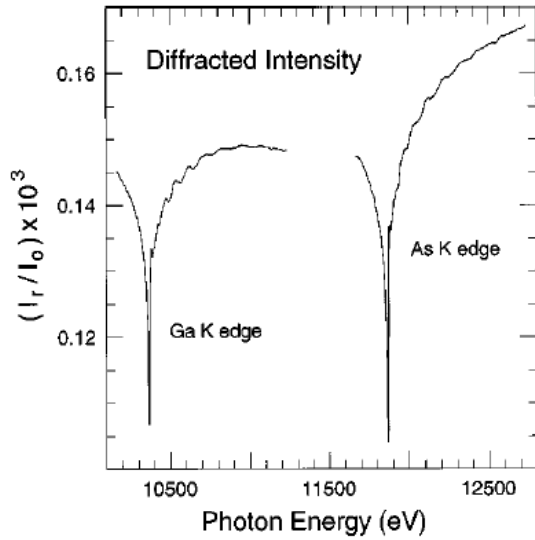


Figure 15: Ga and As K edge DAFS spectra from a buried,  $\text{Ga}_{0.26}\text{In}_{0.74}\text{As}$  alloy grown on a  $\text{GaAs}(001)$  substrate recorded by monitoring the intensity of the  $\text{Ga}_{0.26}\text{In}_{0.74}\text{As}(004)$  Bragg peak. Note the EXAFS-like oscillations in the diffracted intensity that provide the same local structural information as EXAFS.<sup>19</sup>

We will utilize the diffraction anomalous fine structure (DAFS)<sup>18</sup> capabilities of the new NIST BMM beamline that are made possible by having a diffractometer on a scanning XAFS beamline to study both the dimensionality and proximity effects in ferroelectric nano-structures. By combining the spatial specificity of diffraction and its sensitivity to long-range order with the chemical specificity of XAFS and its sensitivity to short-range order, size, shape, and the local atomic structure (and hence the polarization) of ferroelectric nano-crystals will be determined. This is possible because the nano-structures will have unique diffractions in reciprocal space relative to their substrate or host matrix. DAFS has already solved the “common-element” problem for strained-layer superlattices.<sup>19</sup> It has also more recently been applied to the problem of the local structure in self-assembled, embedded nano-particles<sup>17</sup>; i.e., quantum dots embedded in their host matrix. By measuring the ferroelectric spectroscopic signature unique to XAFS by DAFS,<sup>20</sup> we will determine both the amplitude and direction of the ferroelectric polarization as a function of nano-size,<sup>21</sup> shape, proximity, and temperature in these materials that intrinsically possess mixed phases. Comparisons with XAFS

measurements of the corresponding bulk materials under identical conditions will therefore reveal the proximity and dimensionality effects at play in the nano-structures.

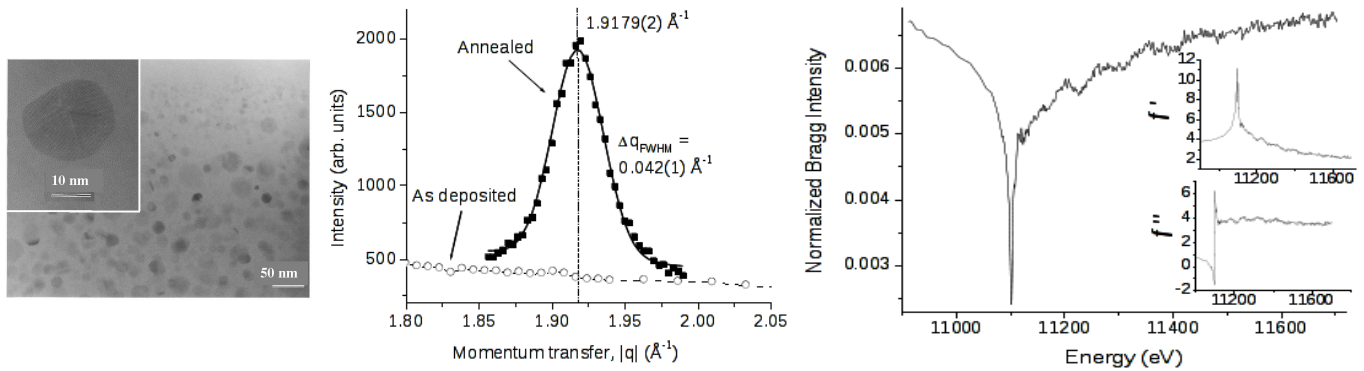


Figure 16: (Left) TEM image of an annealed Ge nano-crystalline sample embedded in  $\text{SiO}_2$ . (Middle) XRD measurements of the  $\text{Ge}(111)$  reflection before and after annealing showing the formation of the nano-crystals. (Right) DAFS from the Ge nano-crystals recorded by measuring the intensity of the  $\text{Ge}(111)$  reflection as a function of energy across the Ge K edge. The inset shows the real and imaginary parts ( $f'$  and  $f''$ ) of the scattering amplitude extracted by a Kramers-Kronig transform.<sup>20</sup>

17 B. Ravel et al, *Ferroelectrics* **206-207**, 407 (1998).

18 H. Stragier, J.O. Cross, J.J. Rehr, Larry B. Sorensen, C.E. Bouldin, and J.C. Woicik, *Phys. Rev. Lett.* **23**, 3064 (1992).

19 J.C. Woicik, E.L. Shirley, C.S. Hellberg, K.E. Andersen, S. Sambasivan, D.A. Fischer, B.D. Chapman, E.A. Stern, P. Ryan, D.L. Ederer, and H. Li, *Phys. Rev. B* **75**, *Rapid Communications*, 140103 (2007).

20 J.C. Woicik, J.O. Cross, C.E. Bouldin, B. Ravel, J.G. Pellegrino, B. Steiner, S.G. Bompadre, L.B. Sorensen, K.E. Miyano, and J.P. Kirkland, *Phys. Rev. B* **58**, *Rapid Communications*, R4215 (1998).

21 A. I. Frenkel, A. V. Kolobov, I. K. Robinson, J. O. Cross, Y. Maeda, and C. E. Bouldin, *Phys. Rev. Lett.*, **89**, 285503 (2002).

## A2: Local Structure Function Relationships in Thin Dielectric Films for Advanced Microelectronics

P. Lysaght (SEMATECH)

SEMATECH has had a six year collaboration with the NIST Synchrotron Methods Group at the NSLS. As a result, SEMATECH's Front End Processing (FEP) Division has conducted state of the art research at each of NIST's three NSLS spectroscopy beamlines for materials' measurements research: X23A2, X24A, and U7A for EXAFS, high-energy XPS, and NEXAFS. This Division has two fundamental technological thrust arenas: *i*) logic and *ii*) memory devices. Both face difficult challenges due to material-limited device scaling. This scenario has placed new demands on virtually every FEP material and unit process, starting with the silicon wafer substrate and encompassing the fundamental planar CMOS building blocks and memory storage structures. The scaling limit of planar bulk CMOS has led to the emergence of MOSFET's employing alternate channel material (Ge or III-V compound semiconductors) in combination with ultra-thin novel metal-oxide dielectric layers uniquely doped to control microstructure driven permittivity for performance enhancement.

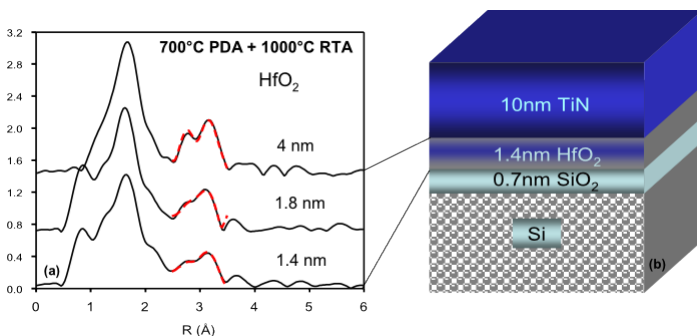


Figure 17: Hf  $L_{III}$  edge EXAFS spectra for three thicknesses of  $HfO_2$  in a  $HfO_2$  gate-stack structure. EXAFS determines the relative concentration of the different phases (microstructure) of the  $HfO_2$  present in the films.<sup>22</sup>

restricted from achieving its lowest free energy state of *m*- $HfO_2$  by physically scaling the dielectric layer from 4.0 nm to 1.4 nm; i.e., the physical thickness of the film did not allow full crystallization into its more energetically stable phase. Consequently, performance advantages have been realized for ultra-thin *t*- $HfO_2$  due to its higher dielectric constant than *m*- $HfO_2$  while model and simulation efforts accurately address the mechanisms responsible for the gate leakage current improvements.

The CMOS gate dielectric (logic) materials example illustrated in Fig. 17 represents one of the numerous material challenges common to advanced device processing. It is comprised of multiple ultra-thin layers of inhomogeneous composition (non-abrupt interfaces), the thermal stability of which must be completely understood.<sup>22</sup> For this reason, Hf  $L_3$  edge EXAFS is an ideal, non-destructive probe of the local atomic structure (and hence  $HfO_2$  phase content) of the sub 2 nm  $HfO_2$  film that is buried beneath the 10 nm TiN electrode. From analysis of the EXAFS data recorded in a glancing incidence geometry above the critical angle, it was determined that the local neighborhood of the  $HfO_2$  is

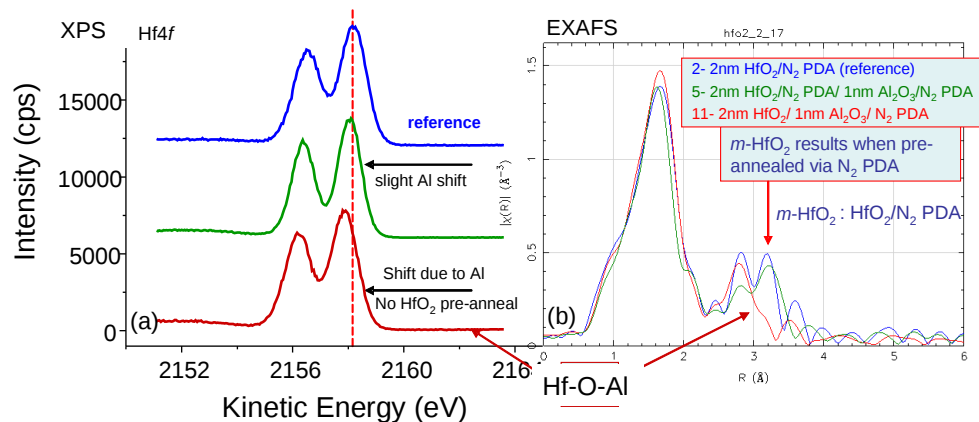


Figure 18: (a) shows a shift to higher binding energy of the Hf 4f photoemission core line due to Al incorporation and the corresponding change of work function. (b) illustrates the EXAFS identification of the amorphous Hf-O-Al network.<sup>16</sup>

HfO <sub>2</sub> / anneal	Monoclinic k = 16-18	Tetragonal k = 28-30
4.0 nm PDA + RTA	0.96	0.04
1.8 nm PDA + RTA	0.6	0.4
1.4 nm PDA + RTA	0.57	0.43

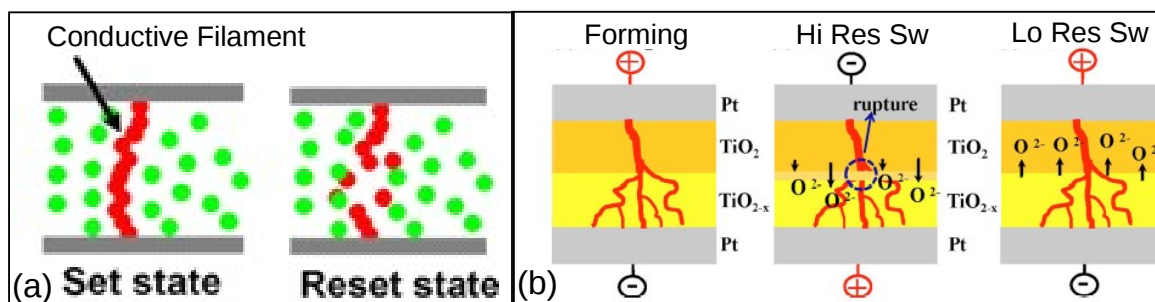
Table 1: The volume fraction of monoclinic (*m*-) and tetragonal (*t*-)  $HfO_2$  polymorphs as a function of film thickness as determined by EXAFS. The samples were measured after device representative thermal budget and reveal the cause of unexpected leakage current improvement for 1.4 nm vs 4.0 nm  $HfO_2$  due to higher dielectric constant (*k*) of *t*- $HfO_2$  compared to *m*- $HfO_2$ .

<sup>22</sup> P.S. Lysaght, J.C. Woicik, M.A. Sahiner, B.-H. Lee, R. Jammy *Appl. Phys. Lett.* **91**, 122910, (2007).

As another example, the microstructure of  $\text{HfO}_2$ -based dielectrics was found to be influenced by Al and La diffusion.<sup>23</sup> This discovery resulted in the ability to tune the effective work function (EWF) of the overlying TiN electrode for both ( $\sim 5$  eV) p-type and ( $\sim 4$  eV) n-type, respectively. Fig. 18 shows the greater work function change (shift of the Hf core level) with Al incorporation as measured by XPS of the Hf 4f core line when the  $\text{HfO}_2$  is not annealed prior to the Al drive-in post deposition anneal (PDA). The EXAFS radial distribution functions of the Hf  $L_3$  edge EXAFS of the same samples show an amorphous-like Hf-aluminate structure corresponding to formation of an Hf-O-Al network. This work demonstrates the power of EXAFS in phase identification of critical electronic thin films for the microelectronics industry and the need for continued collaboration of SEMATECH and NIST.

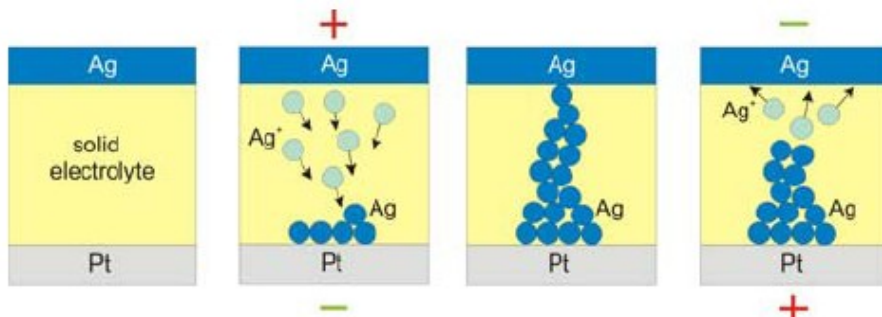
As possible future examples, several new research technologies are emerging for non-volatile random access memories (RAM) offering potential for dense, high speed and lower power memory devices. Operation of most of these technologies is based on employing a resistive element for storing binary data. Of particular interest are those technologies capable of being scaled to and beyond the 16 nm generation. Resistive RAM (RRAM) may derive from different mechanisms that depend strongly on the dielectric(s), stoichiometry, various interfaces, and electrode material. Two such mechanisms that come with significant physical characterization challenges are outlined below.

- 1) Redox: Oxygen / vacancy diffusion to form conductive path or filament.



(a) Oxygen / vacancy diffusion single layer structure.<sup>24</sup> (b) bi-layer structure.<sup>25</sup>

- 2) Substoichiometric, oxygen deficient dielectric layers are designed to rapidly switch coordination as a function of bias voltage. This cycling is proposed to proliferate as dense numbers of local filaments. The potential of RRAM devices to exhibit low-power consumption, high speed, fast operation, high density cross point arrays, etc., makes this design an intriguing advanced replacement for the flash memory common to hand-held portable electronics.



(a) Metallic Ion diffusion forming conductive path or filament.<sup>26</sup>

<sup>23</sup> Lysaght, et al. *International Symposium on Advanced Gate Stack Technology*, (2008).

<sup>24</sup> U. Russo, et al, *IEDM*, VOL. 56, NO. 2, (2009).

<sup>25</sup> Y.H. Do, et al, *Appl. Phys. Lett.* **95**, 093507, (2009).

<sup>26</sup> R. Waser, et al, *ECS Meeting Abstracts* 902, 2149 (2009).



EXAFS at the new NIST NSLS-II BMM will be a suitable probe for such actual working devices fixed in both SET and RESET states. Results will be compared with devices that have been cycled ( $10^6$  x or more) until their lifetime has been exceeded revealing the elusive materials issues that limit device performance.

### A3: EXAFS of Phase Change Materials: Characterizing the role of the Local Bonding Environment on the Crystallization Properties of Chalcogenide Materials for Phase Change Memory Applications

E. Joseph, J. Jordon-Sweet (IBM)

Chalcogenide glass materials have recently garnered significant interest for solid state non-volatile phase change memory applications due to their potential for scalability beyond that of conventional DRAM and Flash memory technologies.<sup>27</sup> These materials undergo rapid crystallization and reamorphization accompanied by orders-of-magnitude changes in resistivity. Such device applications require specific crystallization properties to ensure their crystallization temperature ( $T_x$ ) is sufficiently above standard CMOS device operation ranges ( $\sim 80^\circ\text{C}$ ) but also well below the melting point for thermal stability. Consequently, a thorough understanding of the phase change material system and the role by which the material stoichiometry and local bonding environment affect the crystallization properties are important elements to the optimization of the technology. As an example, significant differences in crystallization speed have been observed for  $\text{Ge}_2\text{Sb}_2\text{Te}_5$  (GST) and chalcogen free materials such as GeSb to which the nucleation mechanism maybe key. (See Fig. 19.)

One method of adjusting material properties is doping of the chalcogenide. Doping favorably modifies crystallization speed, crystallization temperature, and thermal stability. However, the chemical role of the dopant is not always understood. Using X-ray Absorption Fine Spectroscopy (XAFS) at the NIST NSLS-II XAFS and diffraction beamline, one will be enabled to examine the chemical and structural role of the phase change material local bonding environment while concomitantly measuring the diffraction properties of any as-deposited, amorphous and/or crystalline phases.

As an example of previous work, Fig. 20 shows measurements on normalized Ge near edge spectra (A) and Fourier transformed EXAFS spectra (B) for as deposited and annealed  $\text{Ge}_2\text{Sb}_2\text{Te}_5$  (GST) as a function of nitrogen dopant concentration. Measured on NIST beamline X23A2, the data demonstrates that the nitrogen dopant preferentially forms stable Ge-N bonds with shorter bond lengths which are distinct from GST bonds found at longer bond lengths. Furthermore, the local structure of amorphous GST bonds appeared unperturbed by nitrogen addition. Comparing this to the annealed samples (inset), along with the fact that amorphous Ge-N bonds are thermally stable up to  $500^\circ\text{C}$ , while beta- $\text{Ge}_3\text{N}_4$  is stable past  $700^\circ\text{C}$ ,<sup>28</sup> it can be concluded that the Ge-N environment is expected to persist post anneal. In turn, this substantial result leads to the supposition that nitrogen doping does not lead to

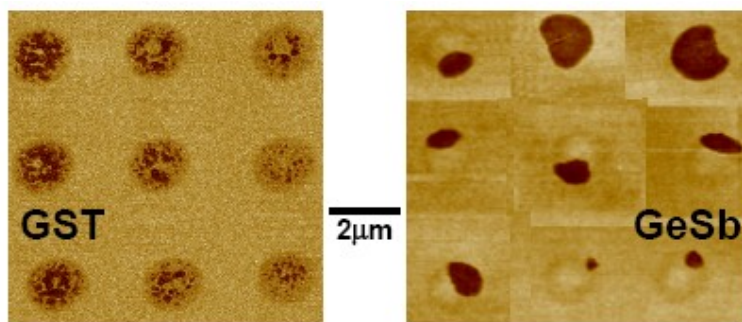
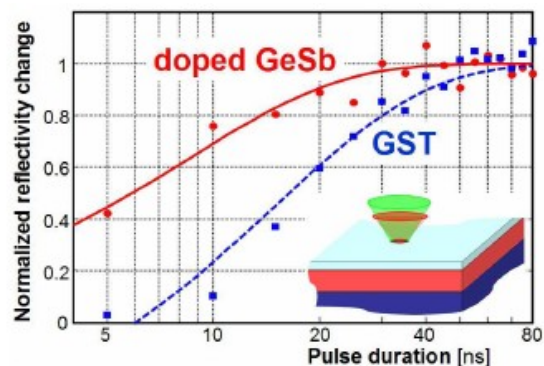


Figure 19: (top) Normalized reflectivity change as a function of optical pulse duration for doped GeSb as compared with undoped GST. Lines show fits to  $1 - \exp(-(t-t_0)/\tau)$ , with a time constant of 8.5 nsec (15 nsec) and a delay time  $t_0$  of 0 nsec (6 nsec) for doped GeSb (GST), respectively. (bottom) AFM images of partially crystallized optical spots in otherwise amorphous as deposited thin films, comparing GST and GeSb via the topography change (darker color) induced during crystallization. In comparison with “nucleation dominated” GST, where crystallization is initiated throughout the optical spot, GeSb is a “growth dominated” phase change material showing only a few nucleation events within each optical spot.<sup>25</sup>

27 Y.C. Chen, C.T. Rettner, S. Raoux *et al.*, IEDM Tech. Dig., p. S30P3, 2006.

28 T. Maeda, T. Yasuda, M. Nishizawa, *et al.*, Appl. Phys. Lett. 85, 3181 (2004).

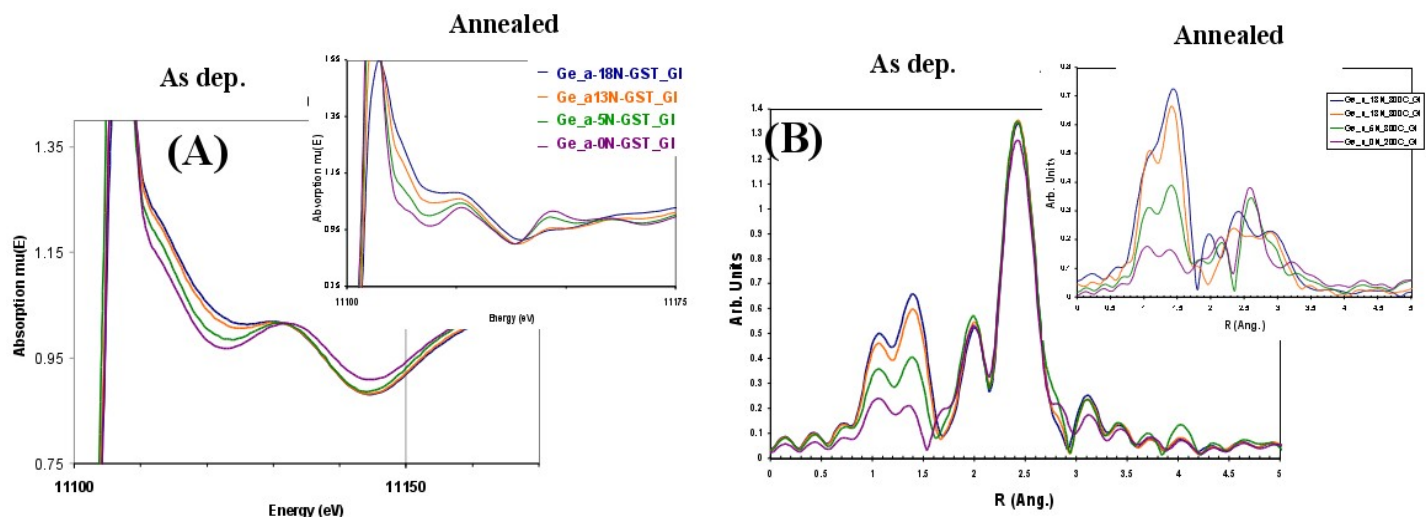


Figure 20: Normalized Ge near edge spectra (A) and Fourier transformed EXAFS (B) of amorphous and crystalline  $\text{Ge}_2\text{Sb}_2\text{Te}_5$  films as a function of nitrogen dopant concentration.

substitution of N into the FCC lattice, nor does it lead to distortion of the FCC lattice, but rather the N dopant instead resides on the grain boundary, where stability and structural nature of Ge-N and Ge-N-Ge bonding refines the grain.<sup>29</sup>

In addition to the role of dopants within the chalcogenide material, combined XAS and XRD also provide a powerful method to understanding phase segregation. Phase segregation has been found to be a prevalent failure mechanism for GeSb based materials and is a major technology issue as it leads to reduced reliability in non-volatile memory applications.<sup>30</sup> An example of phase segregation is shown in Fig. 21 for  $\text{Ge}_{15}\text{Sb}_{85}$  films, where a shift to shorter bond distances is observed as Ge-Sb bonds are replaced by Ge-Ge bonds.

Material modifications such as the addition of specific amounts of tellurium to the material system however, can be advantageous in bridging such networks, ultimately improving phase segregation. Specifically, by measuring Te-doped GeSb 15:85 films using both EXAFS and *in situ* XRD at X23A2 and X20C, it was found that 10% Te addition can significantly prevent the diffusion and phase separation of Ge, most likely related to the Ge-Te bonds formed as-deposited. Addition of 20% Te further produces long range order, resembling the more standard  $\text{Ge}_2\text{Sb}_2\text{Te}_5$  material. An example of this is observed in Figs. 22 and 23 for XRD and EXAFS, respectively.

Although this data provides a great deal of insight into methods of doping and reducing phase segregation of phase change materials, limitations from reduced high energy ( $\sim 30$  keV) photon flux with the NSLS beamline apparatus requires multiple (4-8) hours of data acquisition time per sample and prevents detailed analysis of the Te edge EXAFS data. With the upgrade to the NSLS-II NIST focused XAS and diffraction beamline, coupled with the newly commissioned Si drift detector, it is envisioned that high quality tellurium absorption edge data can be obtained, and all edges of interest can be acquired with improved statistics in a reasonable amount of time, enabling future chalcogenide material learning.

<sup>29</sup> J. S. Washington, Ph.D. Dissertation, NC State University, May 2010

<sup>30</sup> L. Krusin-Elbaum, D. Shakhvorostov, C. Cabral, Jr., S. Raoux, and J. L. Jordan-Sweet, Appl. Phys. Lett. 96, 121906 (2010)

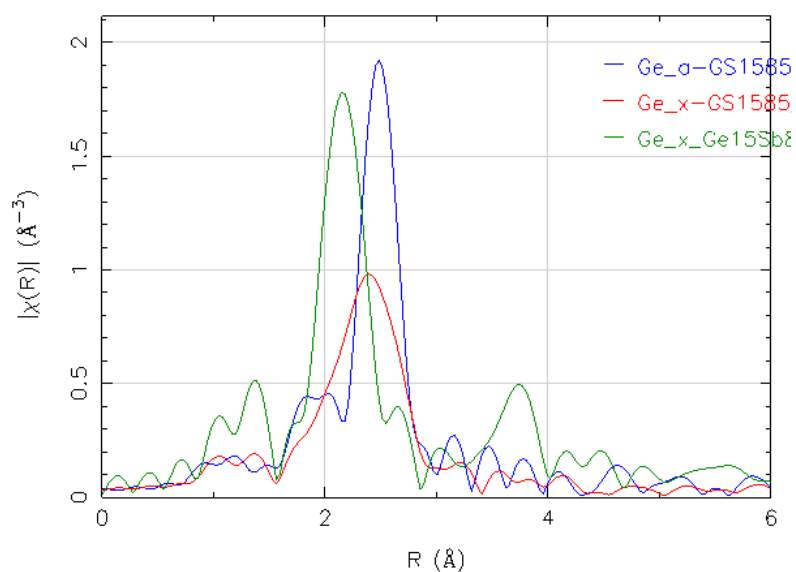


Figure 21: Comparison of the magnitude of the complex Fourier transform of the EXAFS data at the Ge K edge. GeSb 15:85 as deposited (blue line), after a 300°C ramp/quench (red line), and after a 400°C 30 minute anneal (green line).

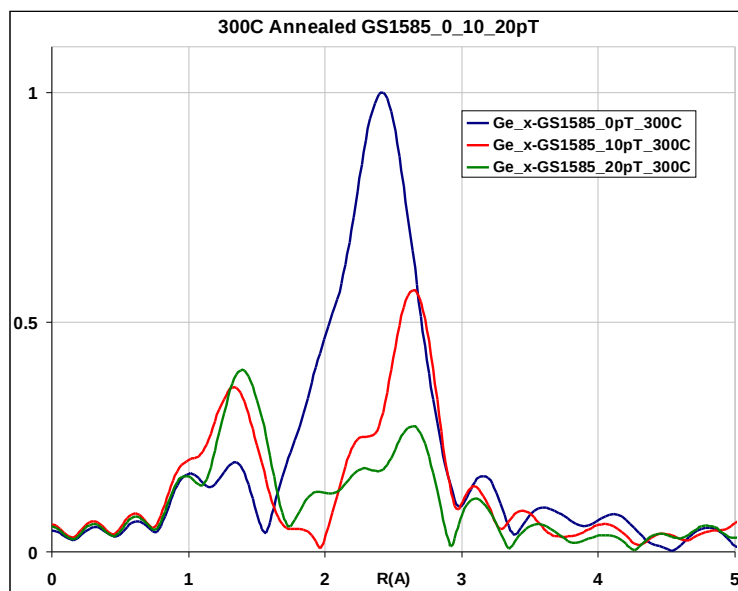


Figure 23: Comparison of the magnitude of the complex Fourier transform of the Ge K edge EXAFS for 300°C annealed 15:85GeSb (blue line), 15:85 GeSb +10% Te (red line), and 15:85 GeSb +20% Te (green line).

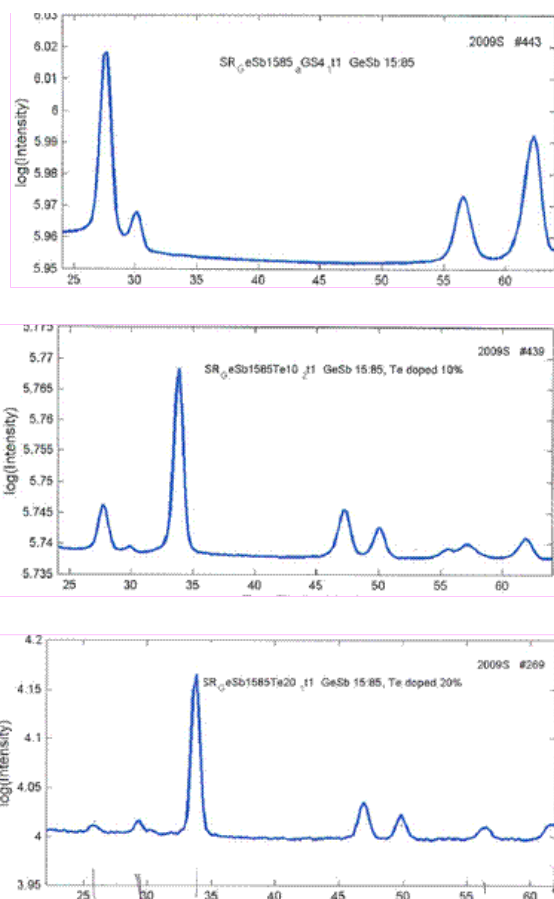


Figure 22: Intensity of diffracted x-ray peaks is plotted vs diffraction angle ( $2\theta$ ) for blanket films of (A) GeSb 15:85, (B) GeSb15:85+10% Te and (C) GeSb 15:85+ 20% Te all heated at a rate of 1°C/s and acquired after a 450°C ramp.



## A.4: High throughput XAS and an example of its application to chemical science

B. Ravel, J.C. Woicik, D. Fischer (NIST)

S.R. Bare, S.D. Kelly (UOP LLC, a Honeywell Company)

Elevated sample throughput and user efficiency is central to the mission of the NIST Beamline for Materials Measurement. Several areas which commonly limit efficiency of XAS measurements will be addressed by this beamline, including:

**Detection:** Detector efficiency is the main rate-limiting step in a fluorescence XAS measurement. We will use silicon drift detectors (SDD) for most fluorescence XAS applications both for ease of use and its superior count rate per element compared to other energy discriminating detectors, recently shown<sup>6</sup> to be above  $4 \cdot 10^5$  counts/second/element with excellent energy resolution.

**Slew scanning:** Replacing the typical step scan used in XAS with a slew scan, a typical XAS measurement time can be reduced by a factor of 2 or more without sacrificing data quality.

**Beamline configuration management:** Many aspects of the beamline must be configured to the energy range of the experiment, including positions of optics and sample stages, ionization chambers gases, and SDD energy window settings. These will be well characterized and recalled from a database, thus greatly reducing downtime during sample changes.

**Data processing:** Effective management of large data sets is another severe throughput limitation of XAS. Sophisticated data archiving and automated post-processing (such as the SDD deadtime correction<sup>6</sup>) will be tightly integrated into the acquisition system.

**High throughput XAS using parallel transmission detection:** Here we show another recent detector development at NIST with significant impact on efficiency and throughput. A novel, four-channel ionization chamber<sup>31</sup> for transmission XAS is used to monitor the temperature evolution of an industrial catalyst under reducing conditions.<sup>32</sup> Productivity and timely response are particularly important in an industrial development program, especially for a project on a fast-track to technology implementation. Here, an alumina-supported nickel oxide catalyst was calcined under various temperatures and atmospheres and from differing precursor materials. Four samples at a time are measured concurrently and under strictly identical conditions in a tube furnace with H<sub>2</sub> gas flow using the parallel detection scheme. The results of one such measurement sequence shown in Fig. 11 display a significant dependence between reduction rate and preparation conditions. In this experiment, the main limit on throughput is the time required to temperature cycle the samples. High measurement throughput is therefore essential to cover a sample set of adequate size to assure relevance to its industrial application. Data processing software has already been developed to handle this increase in data volume. Additional efficiencies would be gained both from the implementation of slew scanning and better beamline configuration management. Ultimately, this approach is applicable to any multi-sample *in situ* experiment or to any apparatus with millimeter-scale spatial variation – for example chemical transformation along the length of a catalytic reactor bed.

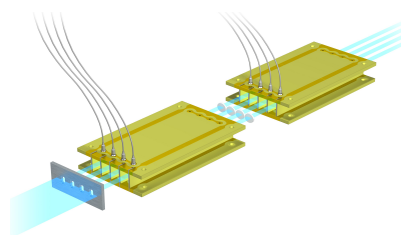


Figure 24: Schematic of a multi-channel ionization chamber for parallel XAS measurement. Image courtesy of UOP.

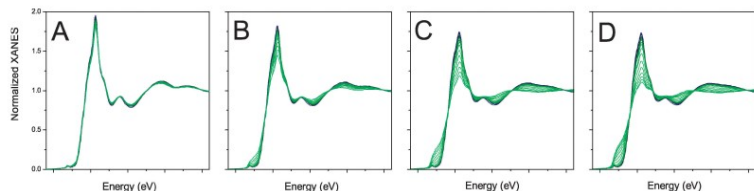


Figure 25: Simultaneous temperature-profiled XANES measurements under identical reducing conditions of a supported nickel catalyst prepared with increasing (A=lowest, D=highest) calcination temperatures. Higher calcination temperatures result in material with faster reduction rates.

31 Ravel et al. *J. Synchrotron Rad.* (2010), **17**, 380-385 [doi:10.1107/S0909049510006230](https://doi.org/10.1107/S0909049510006230)

32 S. Bare et al, *Phys. Chem.Chem. Phys.*, (2010), [doi: 10.1039/b926621f](https://doi.org/10.1039/b926621f)

## Appendix B: Usage statistics at X23A2 and NSLS

*Table 2: X23A2 Users, February 2008 to August 2010*

Name	Institution	# of Visits	Type of user
Simon Bare & Shelly Kelly	UOP	4	Industrial
Jean Jordan-Sweet & Eric Joseph	IBM	4	Industrial
In-Tae Bae	Gillette Technical Center	3	Industrial
Chris Cox	XIA LLC	1	Industrial
Pat Lysaght	Sematech	1	Industrial
Joseph Ziegelbauer	GM Research	1	Industrial
Florian Gstrein & Boyan Boyanov	Intel	1	Industrial
Christophe Adelman	IMEC	1	Foreign Industrial
Igor Levin	NIST	5	PRT
John Sieber	NIST	1	PRT
Lisa Pfefferle & Gary Haller	Yale Univ.	6	Academic
Sarbajit Banerjee	Univ. of Buffalo	4	Academic
Faisal Alamgir	Georgia Tech	3	Academic
Anatoly Frenkel	Yeshiva Univ.	2	Academic
Mehmet Sahiner	Seton Hall Univ.	2	Academic
Dave McKeown	Catholic University	1	Academic
Eric Peterson	Univ. of New Mexico	1	Academic
Natalya Chernova	SUNY Binghamton	1	Academic
Barbara Wilson	Jackson State Univ.	1	Academic
Yongsheng Chen	Penn State Univ.	1	Academic
Helen Hsu-Kim	Univ. of North Carolina	1	Academic
Badri Shyam	George Washington Univ.	1	Academic
Travis Conant	Univ. of New Mexico	1	Academic
Saugata Datta	Kansas State Univ.	1	Academic
Steven Suib	Univ. of Connecticut	1	Academic
Neil Hyatt	Univ. of Sheffield	4	Foreign Academic
Andrea Russel	Univ. of Southampton	2	Foreign Academic
Elise Fox	SREL	1	National Lab
NSLS EXAFS School		2	



STONY BROOK UNIVERSITY  
CHEMISTRY BLDG, ROOM 405  
STONY BROOK, NY 11794-3400  
631-632-8196  
JPSI@SUNYSB.EDU

June 21, 2010

Ladies and Gentlemen:

The Joint Photon Sciences Institute (JPSI) was established at Brookhaven National Laboratory (BNL) and Stony Brook University (SBU) in the fall of 2008. The mission of JPSI is to exploit the properties of advanced photon sources to address the nation's most critical scientific and technical problems. In particular, JPSI will explore the opportunities offered by the unprecedented brightness of the National Synchrotron Light Source II (NSLS-II).

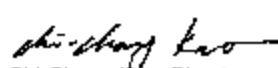
Specifically, JPSI will create an innovative environment where researchers from universities, industries, and government laboratories can work together to identify major scientific and technological opportunities, create device solutions using the most advanced research tools, and catalyze discovery to deployment. The key element of JPSI's strategy is to leverage the presence of thousands of researchers from the more than 400 companies, universities, and government laboratories that carry out research at the NSLS today and will continue to do so at NSLS-II. In addition, JPSI has formed a strategic alliance with the National Institute of Standards and Technology to promote the usage of synchrotrons by industry.

So far, JPSI has focused its program on four themes: microelectronics, energy storage, extreme environments, and solar energy. In each area, leaders from universities, government laboratories and industries were invited to a focused workshop where major technology challenges and capabilities of advanced research tools were presented, new scientific opportunities identified, and collaborative teams formed. These activities have led to major funding from New York State in energy storage, beamline upgrades at the NSLS for microelectronics research, and a new beamline proposal at the NSLS and NSLS-II for advanced lithography. In parallel, JPSI has launched basic research programs in coherent diffraction imaging and nano-diffraction.

As the Directors of JPSI, we are writing in support of the NIST Spectroscopy Beamline Suite: Soft and Tender X-ray Spectroscopy and Microscopy (100 eV to 7.5 keV canted sources), and Hard X-ray Absorption Spectroscopy and Diffraction (4.5 keV to 40 keV three-pole wiggler source) beamline proposal. The proposed beamline is part of the suite of scientific capabilities identified in the four major workshops. It is the intention of JPSI to engage NSLS-II in a partnership agreement to develop these capabilities and to share the stewardship of these beamlines. The aim is to maximize their impact by engaging the intellectual expertise within JPSI and its research partners in these techniques, and to continue to expand these successful research programs at the NSLS today and NSLS-II tomorrow.

Sincerely yours,



  
Chi-Chang Kao, Director

  
John B. Parise, Co-Director

**Name: Daniel A. Fischer**

**Education:** 1984 Physics Ph.D. SUNY, Stony Brook

**Professional Employment:**

*Group Leader (2003-present) Synchrotron Methods, Physicist (1991-present):*  
Ceramics Division, Material Science and Engineering Laboratory,  
National Institute of Standards and Technology

*Physicist:* Exxon Research and Engineering Co., 1984-1991.

*Post Doctoral Research Associate:* City University of New York, 1984.

**Awards:**

- o 2005 *Arthur S. Flemming Award (Scientific Category)*, for pioneering work in developing a critical facility for soft X-ray absorption spectroscopy that has enabled key scientific and technological advances in cutting-edge technology and for groundbreaking work on self-assembled nanoparticles, nanotubes, biomaterials, and high-temperature superconductors.
- o 2004 *Department of Commerce Gold Medal, Individual Award*, for pioneering development of a unique national measurement facility for soft x-ray absorption spectroscopy enabling breakthrough materials advances.
- o 1998 *Department of Commerce Bronze Medal, Group Award*, for leadership and scientific achievement in the development, implementation, and application of advanced x-ray techniques for materials science.
- o 1994 *Department of Commerce Bronze Medal, Individual Award*, for the development of ultra-soft x-ray techniques to measure molecular structure at surfaces and buried interfaces.

**Selected Recent Service to the Scientific Community:**

- 2005-2008: Chair and Vice Chair National Synchrotron Light Source User Executive Committee
- 2006: NSLS User meeting Chair (over 400 attendees, 3 days, 9 workshops)
- 2006-present: Editorial Board Member- Review of Scientific Instruments
- 1998-present: Chair NSLS Vacuum Ultraviolet Proposal Study Panel
- 2007-present: Member NSLS to NSLS II Beamline Transition Working Group

**Over 250 Journal Publications**

**(Below some selected publications; \*Journal Covers and \*NSLS Science Highlights)**

1. \*+ “Enhanced Photovoltaic Properties of Potassium-Adsorbed Titania Nanotubes”, C Richter, C Jaye, D Fischer, L Lewis, R Willey, L Menon, *J. Mater. Chem.*, **19**, 2963–2967 (2009).
2. + “Influence of Dielectric Surface Chemistry on the Microstructure and Carrier Mobility of an n-Type Organic Semiconductor”, P Dhagat, H Haverinen, J Klein, Y Jung, D Fischer, D Delongchamp, G Jabbour, *Adv. Func. Mater.*, **19**, 2365-2372 (2009).
3. + “Enhancement of Engine Oil Wear and Friction Control Performance Through Titanium Additive Chemistry”, J Guevremont, G Guinther, D Szemenyei, M Devlin, T Jao, C Jaye, J Woicik, D Fischer, *Tribol. Trans.*, **51**(3), 324-331 (2008). (*Selected for Editor's Choice Award*)
4. \* “Multilayer mirror fluorescence detection system for photon-in photon-out in-situ carbon K-edge NEXAFS”, D Fischer, S Sambasivan, A Kuperman, Y Platonov, J Wood, *Synch. Rad. News*, **15**, 16-20 (2002).



**Name: Joseph C. Woicik**

**Education/Training:**

Institution and Location	Degree	Year	Field of Study
Stanford University, Stanford CA	Ph.D. and M.S.	1989	Applied Physics
Cornell University, Ithaca NY	B.S.	1983	Applied Physics

**Research and Professional Experience:**

National Institute of Standards and Technology

Senior Physicist	1999-present
Physicist	1991-1999
National Research Council Post Doctoral Fellow	1989-1991

**Professional Activities:**

Spokesperson, beamline X2A2 National Synchrotron Light Source  
Local contact, beamline X24A National Synchrotron Light Source  
Staff member, Advanced Photon Source Sector 33, 2002-2004  
Chair, International Workshop for New Opportunities in Hard X-ray Photoelectron Spectroscopy: HAXPES 2009, Brookhaven National Laboratory, 5/20/09 – 5/22/09  
Chair, Advanced Photon Source Spectroscopy Review Panel, 2003-2005  
Member Advanced Photon Source Beamline Review Panel, 2006  
Member Department of Energy Instrumentation Review Panel, 2007

**Recent Awards:**

Department of Commerce Bronze Metal	1998
-------------------------------------	------

**Selected Publications:**

1. Performance of a 4-element Si drift detector for x-ray absorption fine-structure spectroscopy: Resolution, maximum count rate, dead-time correction, and incorporation into the Athena data analysis software, J.C. Woicik, B. Ravel, D.A. Fischer, and W.J. Newburgh, *J. Synch. Rad.* **17**, 409 (2010).
- 2\*. Oxygen vacancies in N doped anatase TiO<sub>2</sub>: Experiment and first-principles calculations, A.K. Rumaiz, J.C. Woicik, E. Cockayne, H.Y. Lin, G.H. Jaffari, and S.I. Shah, *Appl. Phys. Lett.* **95**, 262111 (2009).
- 3\*\* A ferroelectric oxide made directly on silicon, M.P. Warusawithana, C. Cen, C.R. Slesman, J.C. Woicik, Y. Li, L.F. Kourkoutis, J.A. Klug, H. Li, P. Ryan, L.-P. Wang, M. Bedzyk, D.A. Muller, L.-Q. Chen, J. Levy, and D.G. Schlom, *Science* **324**, 367 (2009).
- 4\*. Phase identification of self-forming Cu-Mn based diffusion barriers on p-SiOC:H and SiO<sub>2</sub> dielectrics using x-ray absorption fine structure, J.M. Ablett, J.C. Woicik, Zs. Tokei, S. List, and E. Dimasi, *Appl. Phys. Lett.* **94**, 042112 (2009).
5. Strain-induced change in local structure and its effect on the ferromagnetic properties of La<sub>0.5</sub>Sr<sub>0.5</sub>CoO<sub>3</sub> thin films, C.K. Xie, J.I. Budnick, W.A. Hines, B.O. Wells, and J.C. Woicik, *Appl. Phys. Lett.* **93**, 182507 (2008).
6. Ferroelectric distortion in SrTiO<sub>3</sub> thin films on Si(001) by x-ray absorption fine structure spectroscopy: Experiment and first-principles calculations, J.C. Woicik, E.L. Shirley, C.S. Hellberg, K.E. Andersen, S. Sambasivan, D.A. Fischer, B.D. Chapman, E.A. Stern, P. Ryan, D.L. Ederer, and H. Li, *Phys. Rev. B* **75**, Rapid Communications, 140103 (2007).
7. Site-specific valence x-ray photoelectron spectroscopy, J.C. Woicik, *Synchrotron Radiation News* **17**, 48 (2004).
- 8\*. Hybridization and bond-orbital components in site-specific x-ray photoelectron spectra of rutile TiO<sub>2</sub>, J.C. Woicik, E.J. Nelson, L. Kronik, M. Jain, J.R. Chelikowsky, D. Heskett, L.E. Berman, and G.S. Herman, *Phys. Rev. Lett.* **89**, 077401 (2002).
9. Direct measurement of valence-charge asymmetry by x-ray standing waves, J.C. Woicik, E.J. Nelson, and P. Pianetta, *Phys. Rev. Lett.* **84**, 773 (2000).
- 10\*. Bond-length distortions in strained-semiconductor alloys, J.C. Woicik, J.G. Pellegrino, B. Steiner, K.E. Miyano, S.G. Bompadre, L.B. Sorensen, T.-L. Lee, and S. Khalid, *Phys. Rev. Lett.* **79**, 5026 (1997).
11. Diffraction anomalous fine structure: A new x-ray structural technique, H. Stragier, J.O. Cross, J.J. Rehr, Larry B. Sorensen, C.E. Bouldin, and J.C. Woicik, *Phys. Rev. Lett.* **23**, 3064 (1992).
12. Studies of Si - Ge interfaces with Surface EXAFS and photoemission, J.C. Woicik and P. Pianetta, in Synchrotron Radiation Research: Advances in Surface and Interface Science: Issues and Technology, Ed. R.Z. Bachrach, 1992 Plenum Press, New York.

**\* NSLS/BNL Highlight**

**\*\* APS/ANL Highlight**

**Name: Bruce Ravel**

**Education/Training:**

Institution and Location	Degree	Year	Field of Study
University of Washington	Ph.D	1997	Physics
Wesleyan University	B.A.	1989	Physics ( <i>magna cum laude</i> )

**Research and Professional Experience:**

National Institute of Standards and Technology

Scientist, Synchrotron Measurement Group	Nov. 2007-present
National Research Council Postdoctoral Fellow	1997-1999

Argonne National Laboratory

Physicist, Biology Division	2005-2007
-----------------------------	-----------

Naval Research Laboratory

Physicist, Chemistry Division	2001-2005
-------------------------------	-----------

Centre Nationale de la Recherche Scientifique

Visiting scientist	2000-2001
--------------------	-----------

**Professional Activities:**

- Beamline experience
  - Local contact, beamline X23A2 2007-present
  - Staff member, APS Sector 10, 2005-2007
  - Spokesperson, beamlines X11A, X11B, X23B, 2003-2005
- Committees
  - Executive committee member, International X-ray Absorption Society, 2005-present
  - Chair, NSLS User Executive Committee, 2009-2010
- XAS software and education
  - Organizer/instructor XAS Schools: NSLS (2003-2005, 2008, 2009), APS (2006-2009), SLS (2007,2009), Thai Synchrotron (2009,2010), University of Alberta (2005), Polish Academy of Science (2006), University of Ghent (2010)
  - Co-author of the *IFEFFIT* package, a widely used package for XAS data analysis, 2001-present
  - Contributing author of *FEFF8*, a widely used XAS theory program
- Review Panels
  - Proposal Review Panel, National Synchrotron Light Source, 2007-present
  - Proposal Review Panel, Advanced Photon Source, 2006-present
  - Proposal Review Panel, Canadian Light Source, 2006-present

**Selected Publications:**

1. *ATHENA, ARTEMIS, HEPHAESTUS: data analysis for X-ray absorption spectroscopy using IFEFFIT*, B. Ravel and M. Newville, *J. Synchrotron Rad.* **12**, pp. 537-541 (2005), [doi:10.1107/S0909049505012719](https://doi.org/10.1107/S0909049505012719)  
At 706 citations, this is the most frequently cited article from The Journal of Synchrotron Radiation.
2. *Real Space Multiple Scattering Calculation and Interpretation of X-Ray Absorption Near Edge Structure*, A.L. Ankudinov, B. Ravel, J.J. Rehr, and S. Conradson, *Phys. Rev* **B58**, #12, pp. 7565-7576, (1998), [doi: 10.1103/PhysRevB.58.7565](https://doi.org/10.1103/PhysRevB.58.7565)
3. *Simultaneous XAFS measurements of multiple samples*, B. Ravel, C. Scorzato, D.P. Siddons, S.D. Kelly, S.R. Bare, J. Synchrotron Radiat., **17** (2010) 380-385, [doi:10.1107/S0909049510006230](https://doi.org/10.1107/S0909049510006230)
4. *Performance of a four-element Si drift detector for X-ray absorption fine-structure spectroscopy: resolution, maximum count rate, and dead-time correction with incorporation into the ATHENA data analysis software*, J.C. Woicik, B. Ravel, D.A. Fischer, W.J. Newburgh, *J. Synchrotron Radiat.*, **17** (2010) 409-413, [doi:10.1107/S0909049510009064](https://doi.org/10.1107/S0909049510009064)
5. *The structure of ion beam amorphised zirconolite studied by grazing angle X-ray absorption spectroscopy*, D.P. Reid, M.C. Stennett, B. Ravel, J.C. Woicik, N. Peng, E.R. Maddrell and N.C. Hyatt, *Nuclear Instruments and Methods in Physics Research B* **268**:11-12, (2010) 1847-18521, [doi:10.1016/j.nimb.2010.02.026](https://doi.org/10.1016/j.nimb.2010.02.026)
6. *Condensed Matter Astrophysics: A Prescription for Determining the Species-specific Composition and Quantity of Interstellar Dust Using X-rays*, J.C. Lee, J. Xiang, B. Ravel, J. Kortright K. Flanagan, *The Astrophysical Journal* **702**:2 (2009) 970, [doi: 10.1088/0004-637X/702/2/970](https://doi.org/10.1088/0004-637X/702/2/970)
7. *Protein Oxidation Implicated as the Primary Determinant of Bacterial Radioresistance* M. J. Daly, E. K. Gaidamakova, V. Y. Matrosova, A. Vasilenko, M. Zhai, R. D. Leapman, B. Lai, B. Ravel, S.-M. W. Li, K. M. Kemner, J. K. Fredrickson *PLOS Biology* **5**:4, (2007), [doi:10.1371/journal.pbio.0050092](https://doi.org/10.1371/journal.pbio.0050092)